Solar Energy 259 (2023) 348–355

Contents lists available at ScienceDirect

Solar Energy

journal homepage: www.elsevier.com/locate/solener

Excellent surface passivation of p-type TOPCon enabled by ozone-gas oxidation with a single-sided saturation current density of ~ 4.5 fA/cm^2

Na Lin [a,b], Zhenhai Yang [b], Haojiang Du [b], Zetao Ding [b], Zunke Liu [b], Haiyang Xing [b], Mingjing Xiao [b], Yali Ou [a,b], Wei Liu [b], Mingdun Liao [b], Baojie Yan [b], Shihua Huang [a,*], Yuheng Zeng [b,*], Jichun Ye [b,*]

[a] Provincial Key Laboratory of Solid State Optoelectronic Devices, Zhejiang Normal University, Jinhua 321004, Zhejiang Province, China
[b] Zhejiang Provincial Engineering Research Center of Energy Optoelectronic Materials and Devices, Ningbo Institute of Materials Technology & Engineering, Chinese Academy of Sciences, Ningbo 315201, China

ARTICLE INFO

Keywords:
Ozone gas (O_3) oxidation
p-Type TOPCon
Boron-doped polysilicon
Passivation quality
PECVD

ABSTRACT

High-quality p-type tunnel oxide passivated contact (p-type TOPCon) is a feasible technical solution to further improve the efficiency of TOPCon silicon solar cells. Plasma-enhanced chemical vapor deposition (PECVD) technology route could deposit boron-doped amorphous silicon film in-situ and thus becomes one of the most promising industry routes to prepare the TOPCon structure. However, the passivation quality of p-type TOPCon by PECVD is not satisfactory till now. In this work, we develop the high-performance p-type TOPCon technology by integrating the ozone-gas oxidation to prepare the ultra-thin SiO_x film, which shows excellent passivation and contact properties. The experimental results suggest that the double-sided p-type TOPCon passivated samples with p-type Si substrates receive a maximal implied open-circuit voltage (iV_{oc}) of ~ 734 mV together with a minimum single-sided saturation current density ($J_{0,s}$) of ~ 4.5 fA/cm^2. Correspondingly, the contact resistivity is less than 5 mΩ·cm^2, yielding a high selectivity S_{10} of 15.6, which is one of the best values for p-type TOPCon technology. As a result, the precursor cell manifests an excellent iV_{oc} of 717 mV, and the p-type silicon solar cell with rear-sided p-type TOPCon passivating contact receives a high efficiency of 22.23%. Generally, this work provides a promising technology for preparing the high-quality p-type TOPCon passivating contact for industrial application.

1. Introduction

Tunnel Oxide Passivated Contact (TOPCon) technology has gained widespread recognition as the most promising photovoltaic (PV) technology for the next generation of high-efficiency silicon (Si) solar cells (SCs). It is compatible with the existing Passivated Emitter and Rear Contact (PERC) SCs in production lines [1,2–3,5,10]. At present, the n-type TOPCon technology (n-type TOPCon) is developing rapidly with high efficiency. For example, Fraunhofer ISE achieves a lab-scaled n-type TOPCon SCs with a high efficiency of 25.8% by optimizing the resistivity and thickness of the silicon wafer [18]. The leading companies have realized mass-production efficiencies of 24.5%−25.5% [15]. Despite advancements in technology, the cost of producing n-type Si SCs remains higher than that of p-type cells. This is due to several factors, including the expensive n-type silicon wafer, boron diffusion process, and rear Ag paste, and so on [4].

P-type TOPCon based on p-type Si wafers has the potential to achieve both high-efficiency and low-cost for SCs. Since the efficiency of the PERC SCs is limited by the direct contact of rear aluminum (Al) electrodes and silicon substrates, the p-type TOPCon SCs could detour this issue by the full-area passivation and contact design, which thus could receive higher implied open-circuit voltage (iV_{oc}) and fill factor (*FF*). In addition, the p-type TOPCon cells can utilize the mature phosphorus diffusion process and low-penetration aluminum electrode technology, showing a low-cost technology route. Another advantage of p-type TOPCon SCs is that they can be produced on existing PERC technology production lines with just a few additional manufacturing equipments. This is also one of the important reasons for the ready acceptance of this technology in industry [2]. More importantly, the p-type TOPCon structure could also work as a core component to construct high-

* Corresponding authors.
E-mail addresses: huangshihua@zjnu.edu.cn (S. Huang), yuhengzeng@nimte.ac.cn (Y. Zeng), jichun.ye@nimte.ac.cn (J. Ye).

https://doi.org/10.1016/j.solener.2023.05.028
Received 5 March 2023; Accepted 18 May 2023
Available online 29 May 2023
0038-092X/© 2023 International Solar Energy Society. Published by Elsevier Ltd. All rights reserved.

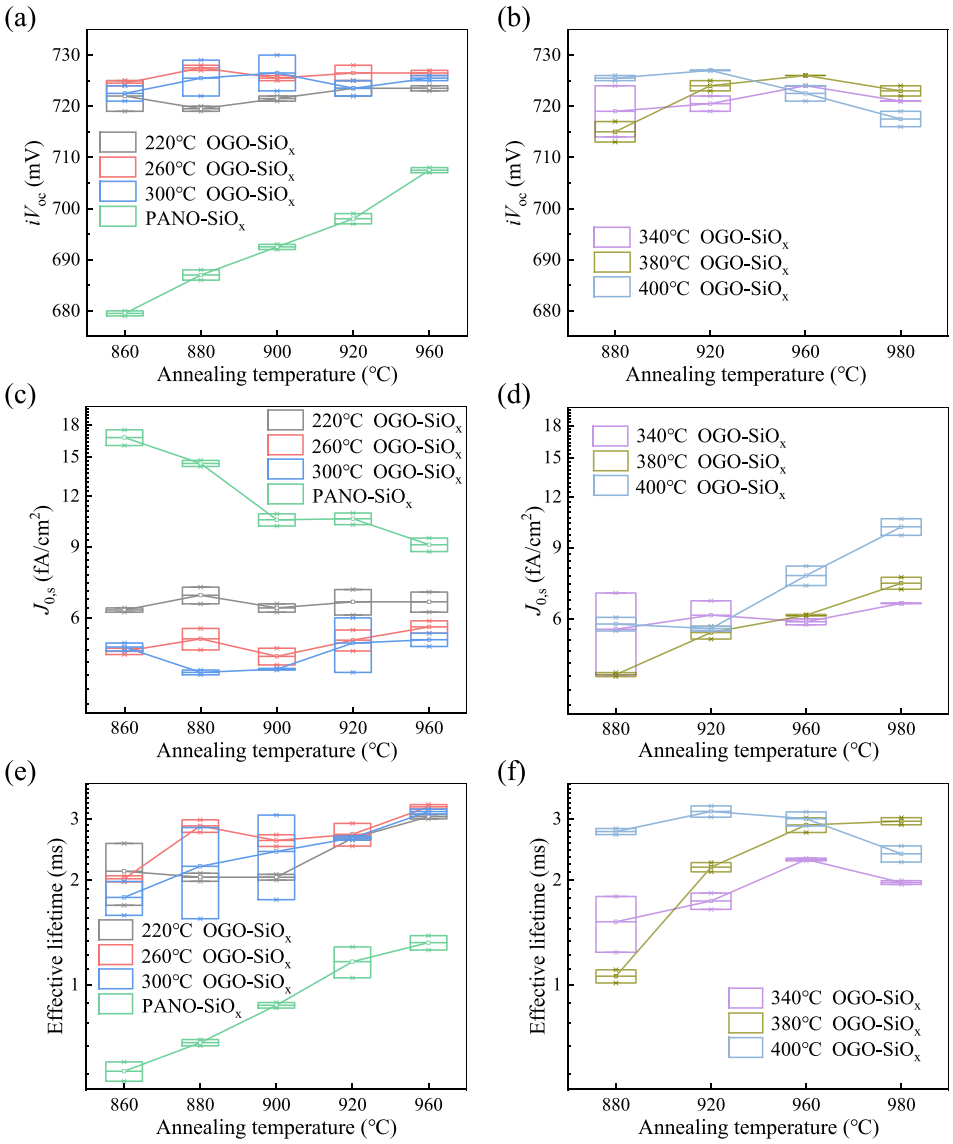

Fig. 1. The passivation performance of p-type TOPCon samples with OGO-SiO$_x$ and PANO-SiO$_x$ under different oxidation and annealing temperatures was evaluated through (a)-(b) iV_{oc}, (c)-(d) $J_{0,s}$, and (e)-(f) τ_{eff}.

efficiency TOPCon SCs, such as p-type polarity for the back contact SCs, the front-sided poly-finger for the n-type TOPCon SCs, and the p-type emitter for the back junction n-type SCs.

Low-pressure chemical vapor deposition (LPCVD) is widely used to manufacture TOPCon SCs [8]. Fraunhofer ISE has achieved high-quality passivation with a high iV_{oc} of 737 mV and a low single-sided saturation current density ($J_{0,s}$) of 2 fA/cm^2 using wet silicon oxide and LPCVD in-situ boron-doped amorphous silicon (B-doped a-Si:H) [22]. However, the LPCVD technology route also suffers from many drawbacks, such as low deposition rate, wrap-around deposition, non-uniformity, and the frequent replacement of quartz components *etc*., making it difficult from being adopted by the industry. As a more promising alternative technology, plasma-enhanced chemical vapor deposition (PECVD) has also been widely developed due to its remarkable advantages in deposition rate, versatility, wrap-free deposition, and ease of cleaning. In order to fully realize the potential of PECVD technology, various institutions have focused on developing this technology and have achieved significant progress with p-type TOPCon structures. For instance, in 2014, Fraunhofer ISE reported the fabrication of TOPCon structures with an iV_{oc} of 680 mV and a $J_{0,s}$ of 50 fA/cm^2 [5]. In 2018, EPFL utilized very-high-frequency PECVD (VHF-PECVD) to deposit TOPCon samples with an iV_{oc} of 715 mV and a $J_{0,s}$ of 11 fA/cm^2 [13]. In 2020, NIMTE achieved high-level passivation with an iV_{oc} of 722 mV and a $J_{0,s}$ of 6 fA/cm^2 through thermal oxidation SiO$_x$ (TO-SiO$_x$) [11]. Most recently, in 2022, they used a two-step oxidation method to achieve a high iV_{oc} of 712 mV and a low $J_{0,s}$ of 10 fA/cm^2 [16,25].

Despite many progresses have been made, the use of PECVD for the p-type TOPCon is still challenging due to the difficulty of achieving high-quality passivation at the current stage. It is confirmed that the simple regulation of the parameters/conditions of the deposition of B-doped a-Si:H through PECVD alone cannot significantly promote the passivation quality of p-type TOPCon. TO-SiO$_x$ has been confirmed to provide the highest quality passivation compared with other types of SiO$_x$. However, such a TO-SiO$_x$ often requires a high deposition temperature (about 600 °C), making it impossible to use the industrial graphite boats. Therefore, it is important to develop a low-temperature PECVD technology for p-type TOPCon. Our previous work has shown that ozone gas oxidation (OGO) that is compatible with industrial graphite boats could achieve low-temperature oxidation, providing a practical and effective way to improve the passivation performance of the industrial n-type TOPCon SCs[15].

Inspired by the application of ozone gas oxidation in n-type TOPCon

SCs, we investigated the potential of utilizing ozone gas oxidation technology in conjunction with PECVD to fabricate the high-performance p-type TOPCon. Through careful optimization of the oxidation conditions, high-quality p-type TOPCon with a remarkable iV_{oc} of 734 mV, a $J_{0,s}$ of 4.5 fA/cm^2, and a low contact resistivity (ρ_c) of less than 5 mΩ·cm^2 was achieved, suggesting a promising maximum selectivity (S_{10}) of 15.6. Furthermore, we fabricated precursor p-type TOPCon SCs with an iV_{oc} of 717 mV, which could lead to a high V_{oc} of approximately 710 mV if the metallization process can be well-controlled, demonstrating the viability of the technology to achieve high-performance p-type TOPCon SCs. Our proof-of-concept p-type TOPCon SCs demonstrated an impressive efficiency of 22.23%, validating the potential of utilizing ozone-gas oxidation technology in combination with PECVD to produce high-efficiency p-type TOPCon SCs.

2. Experimental details

2.1. Preparation and characterization of the p-type TOPCon lifetime samples

Passivation samples were prepared using planar p-type CZ c-Si wafers, which had a thickness of 165 μm and a resistivity (R) range of 3–6 Ω·cm. The wafers were first polished with alkaline, followed by standard RCA cleaning. The ozone gas was prepared by the high concentration ozone generator, and flowed into the diffusion furnace (74 mm × 1000 mm) under ozone concentration of 400 mg/L. The silicon wafers were immersed in 5 vol% HF solution to remove the as-grown oxide, then put into the furnace for oxidation. The oxidation temperature was varied from 220 °C to 400 °C with a dwell time of 10 min. Meanwhile, the comparison samples were oxidized via PANO in an RF PECVD system at 150 °C. Subsequently, a 30 nm layer of boron-doped amorphous silicon was deposited on both sides of the two types of ultra-thin SiO_x coated wafers using an RF PECVD system. The amorphous Si crystallization and B activation were realized by high temperature N_2 annealing at 800–1000 °C for 30 min, followed by the wet N_2 hydrogenation process [24]and then the aluminum oxide hydrogenation.

The photo-conductance decay (PCD) can be measured by Sinton WCT-120 from which τ_{eff}, iV_{oc} and $J_{0,s}$ for passivation quality characterization can be attained. The chemical bonding structure and oxide layer thickness of SiO_x layer were analyzed by the angle-resolved XPS (ARXPS). The extract density of interface state (D_{it}) was determined by performing high frequency (1 MHz) capacitance–voltage (C-V) analysis on the metal–insulator-semiconductor (MIS) structure using a semiconductor characterization system (Keithley-4200-SCS). To measure the dopant concentration profiles, we used an electrochemical C-V measurement system (Buchanan, CVP21). Using the EDNA2 program, the diffusion current density ($J_{0,diffusion}$) was estimated based on the dopant concentration profiles. The Cox-Strack (C-S) method was used to measure the ρ_c of the poly-Si/SiO_x/c-Si junctions. The metal disks were formed by metal evaporation.

2.2. Fabrication of the p-type TOPCon SCs

The cell samples were fabricated using p-type Ga-doped CZ c-Si wafers, which had a thickness of 170 μm and a resistivity of approximately 1 Ω·cm. The front surface was etched using KOH to create a randomly textured surface, followed by phosphorus diffusion. The back surface was treated with acid polishing. After being cleaned by RCA solutions, the wafers were put into the diffusion furnace to be oxidized by ozone gas at 400 °C for 10 min, followed by deposition of 30 nm B-doped a-Si:H on the rear side. After high-temperature annealing for crystallization and activation, SiN_x was deposited on the front by PECVD, and the front anti-reflection layer was formed. The seed layer for the front electrode, consisting of Ti/Pd/Ag, was prepared using electron beam deposition, while the full-side rear Ag electrode was prepared using thermal evaporation. The front electrode was then thickened by silver plating. A layer of MgF_2 was deposited onto the front side using thermal evaporation to enhance its anti-reflection properties.

The efficiency of the SCs was tested at 25 °C and AM1.5 using a solar simulator (Enlitech, SS-F5-3A), while the electrical performance was evaluated using Suns-V_{oc}. To measure the EQE of the SCs, we used the EQE system (Enlitech, QE-R3011).

3. Results and discussion

The quality of the tunnel oxide film is highly dependent on the oxidation and annealing temperatures used during ozone gas oxidation. Fig. 1 compares the passivation performance of AlO_x hydrogenation under different oxidation and annealing temperatures of ozone gas oxidation with plasma-assisted N_2O oxidation (PANO), which is commonly used. From these passivation properties in Fig. 1, we can find that:

1) Fig. 1 illustrates the impact of oxidation and annealing temperatures on the passivation performance of AlO_x hydrogenated tunnel oxide films. As seen in Fig. 1(a, b), the iV_{oc} values with OGO-SiO_x exhibit an increasing trend with increasing annealing temperature, except for the 220 °C OGO-SiO_x sample. However, the differences in iV_{oc} values are relatively small, indicating that OGO-SiO_x passivation quality is tolerant to oxidation and annealing temperatures. The best passivation performance with an iV_{oc} of 730 mV is achieved at an oxidation temperature of 300 °C and an annealing temperature of 900 °C. In contrast, the iV_{oc} values with PANO-SiO_x increase monotonically from 680 mV to 710 mV with increasing annealing temperature from 860 °C to 960 °C, suggesting a narrower annealing window and relatively lower passivation performance of PANO-SiO_x compared to OGO-SiO_x. The poorer passivation of PANO-SiO_x samples can be attributed to the plasma bombardment damage during the plasma-assisted N_2O oxidation process.
2) The $J_{0,s}$ values under the different cases were plotted in Fig. 1(c, d), which show the similar variation trend with that of iV_{oc} values in Fig. 1(a, b). Specially, a lower oxidation temperature would lead to the insufficient oxidation, resulting in a higher $J_{0,s}$, while a higher oxidation temperature has a negative effect on $J_{0,s}$ because the overly high temperature may cause thermal decomposition of OGO-SiO_x. As a result, the optimal $J_{0,s}$ with a value of 4.3 fA/cm^2 is achieved under the oxidation temperature of 300 °C and annealing temperature of 880 °C.
3) The effective lifetimes of OGO-SiO_x samples were summarized in Fig. 1(e, f). The results indicate that OGO-SiO_x samples exhibit superior passivation, as evidenced by a best lifetime of 3.3 ms.
4) The passivation performance of samples with OGO-SiO_x show a great tolerance for oxidation and annealing temperatures. Furthermore, the oxidation temperature of below 400 °C discussed in this study could be suitable for integration into existing production lines that use graphite boat as the deposition carrier.
5) The optimal annealing temperature of OGO-SiO_x was achieved at 860–880 °C, which is far below that of PANO-SiO_x. This means that the use of OGO-SiO_x in p-type TOPCon cells can achieve superior passivation performance with a higher iV_{oc}, and lower thermal budge due to the relatively lower annealing temperature required. This minimizes the impact of high-temperature annealing on the P profile of the emitter and allows for the production of highly efficient p-type TOPCon cells.

To uncover the effect of oxidation process of OGO-SiO_x on the passivation performance, we evaluate the residence times (t_{res}) of ozone gas in the furnace tube[6]. The t_{res} of gas inside a tube can be calculated by the following equation: $t_{res} = F_{in}/V_{tube}$, where F_{in} is the gas volume flow and V_{tube} is the volume of the tube. By applying the ideal gas law ($PV = nRT$, where P is pressure, V is volume, n is the number of moles, R

Table 1
Ozone gas residence times (t_{res}) under the different oxidation temperatures. (Gas flow is 1 slm; pressure is 1 atm; diameter and length of tube are 7.4 and 100 cm, respectively.).

Oxidation temperature (°C)	200	260	300	340	380	400
Residence time (sec)	150	136	123	118	111	105

is the universal gas constant, and T is the absolute temperature), we can calculate the volume of gas that enters the tube. Table 1 shows that the ozone gas t_{res} in our small tube ranges from 150 to 105 sec at temperatures of 200–400 °C. The t_{res} inside the tube is significantly higher than the lifetime of ozone gas, which allows for the production of high-quality nano SiO_x layer and p-type TOPCon [6]. It is worth noting that we have previously prepared nano SiO_x with ozone gas oxidation in a large industrial tube (tube diameter 52.8 cm × length 300 cm, 100 Pa, 8 SLM) [15], in which the t_{res} of ozone gas is about 2.5 sec at 260 °C and 2.0 sec at 400 °C. The t_{res} of ozone gas in the industrial tube is lower than in the small tube, but still maintains an effective concentration for preparing high-quality nano SiO_x layer and p-type TOPCon. A previous study has confirmed the successful achievement of excellent n-type TOPCon with maximum iV_{oc} using ozone gas oxidation in a large tube [15]. Therefore, we conclude that OGO technology is feasible for preparing nano SiO_x for TOPCon structures in larger industrial tubes.

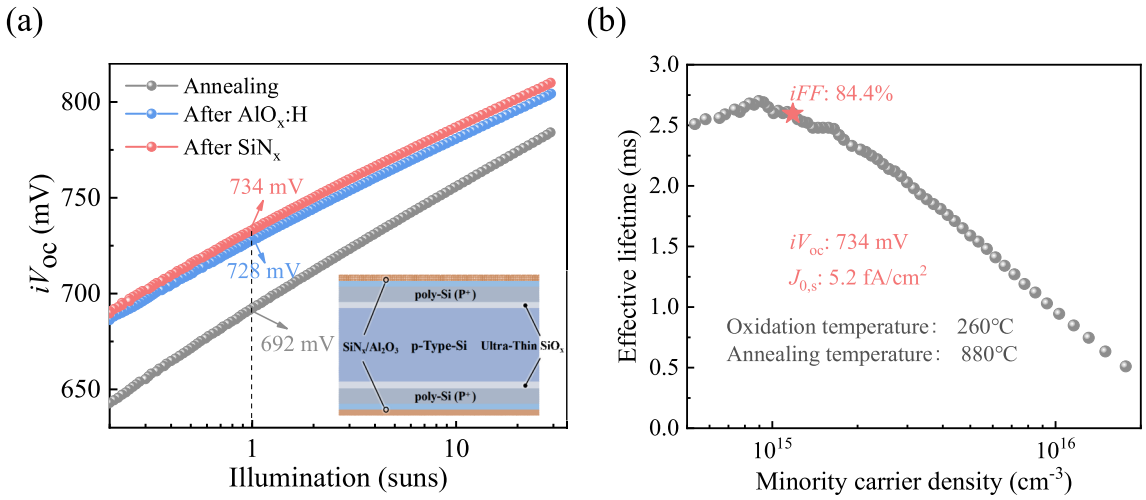

Fig. 2. (a) Illumination-dependent iV_{oc} under the different cases, where the corresponding measure structure was also inserted. (b) Effective lifetime curve of the highest passivation sample, in which τ_{eff}, iV_{oc}, $J_{0,s}$ and iFF values were also marked in the figure.

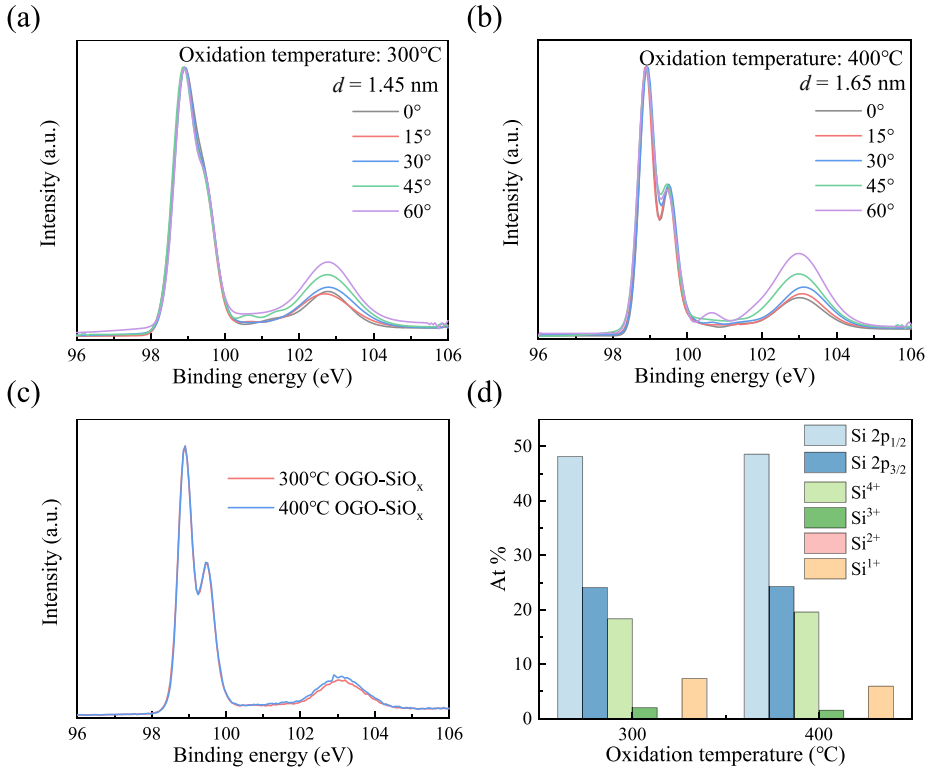

Fig. 3. Thickness-dependent ARXPS for OGO-SiO_x at the oxidation temperature of (a) 300 °C and (b) 400 °C. (c) XPS spectra of the corresponding samples under an incident angle of 0. (d) The sub-stoichiometric Si species of XPS spectra in Fig. 3(c).

Table 2
Statistics of sub-stoichiometric Si species ratios in the different oxidation temperatures.

Oxide Temperature Peak position (eV)	Si^{4+} ratio (%) (102.3–103.7)	Si^{3+} ratio (%) (101.38)	Si^{2+} ratio (%) (100.65)	Si^{1+} ratio (%) (99.85)
300 °C	~18.4	~2.0	~0	~7.4
400 °C	~19.6	~1.5	~0.1	~6.0

To further enhance the passivation quality of OGO-SiO_x samples, a SiN_x capping layer was applied to cover the passivation wafers. The inset in Fig. 2(a) depicts the passivation structure, while Fig. 2(a, b) displays the optimal passivation results. It can be observed that, compared to the AlO_x hydrogenation with an iV_{oc} of 728 mV, the sample with the additional SiN_x capping layer shows a higher iV_{oc} of 734 mV. For the samples with 260 °C oxidation, 880 °C annealing and SiN_x caping, the optimal passivation was characterized by iV_{oc} of 734 mV, $J_{0,s}$ of 5.1 fA/cm^2, and τ_{eff} of 2.6 ms. Additionally, the corresponding implied fill factor (*iFF*) was calculated to be 84.4%, indicating that a high potential of fabricating high performance p-type TOPCon SCs.

We have demonstrated in this study that ozone gas can be used for the deposition of silicon oxide, resulting in high-quality p-type TOPCon at a wide range of oxidation and annealing temperatures. By combining with the industrialized tube PECVD, one can realize the two-in-one preparation of silicon oxide and polysilicon [15]. Compared to our previous study, which used PANO-SiO_x to prepare passivation samples with a best iV_{oc} of 722 mV, $J_{0,s}$ of 6 fA/cm^2, OGO-SiO_x method shows higher passivation with an optimal iV_{oc} of 734 mV, $J_{0,s}$ of 5.2 fA/cm^2. Furthermore, a two-step oxidation method combining pre-deposition of wet chemical SiO_x with plasma oxidation was used to suppress ion bombardment, leading to an excellent iV_{oc} of 712 mV and a $J_{0,s}$ of ~ 12 fA/cm^2 was achieved [16]. The ozone oxidation method still provides the best passivation quality for the p-type TOPCon.

To uncover the high passivation of p-type TOPCon with OGO-SiO_x, we conducted XPS analysis on silicon oxide film, where two typical oxidization temperature (i.e., 300 °C and 400 °C) were considered. Fig. 3 (a, b) displays ARXPS curves under the oxidization temperature of 300 °C and 400 °C, respectively. The thickness and composition of the nano-sized silicon oxide layer can be accurately determined by detecting signals at different depths using varying emission angles [17]. During the XPS measurement, five emission angles in the vertical incidence direction, i.e., 0°, 15°, 30°, 45° and 60° were considered. The SiO_x thicknesses were determined by XPS analysis to be 1.45 nm and 1.65 nm for oxidation temperatures of 300 °C and 400 °C, respectively. The intensity of the Si^{4+} peak in Fig. 3(c) was higher for the sample oxidized at 400 °C than for that oxidized at 300 °C, suggesting an improved oxidation ability of the silicon oxide formed on the p-type silicon substrates with increasing oxidation temperature. Fig. 3(d) and Table 2 present the content ratios of peak deconvolution, where the OGO-SiO_x under 400 °C oxidation shows lower content ratio of the sub-stoichiometric Si but higher content ratio of the stoichiometric Si (*i.e.*, 19.6 at.% for Si^{4+}) compared with that of 300 °C OGO-SiO_x (*i.e.*, 18.4 at.% for Si^{4+}), hinting that higher oxidation temperature would lead to the thicker SiO_x and higher Si^{4+} content. Our previous work showed that the Si^{4+} content of ozone gas based SiO_x at 260 °C oxidation was 19.6 at.%, which is consistent with the result of this work. However, apart from the oxidation temperature, the passivation performance of such a p-type TOPCon with OGO-SiO_x is also affected by annealing temperature and

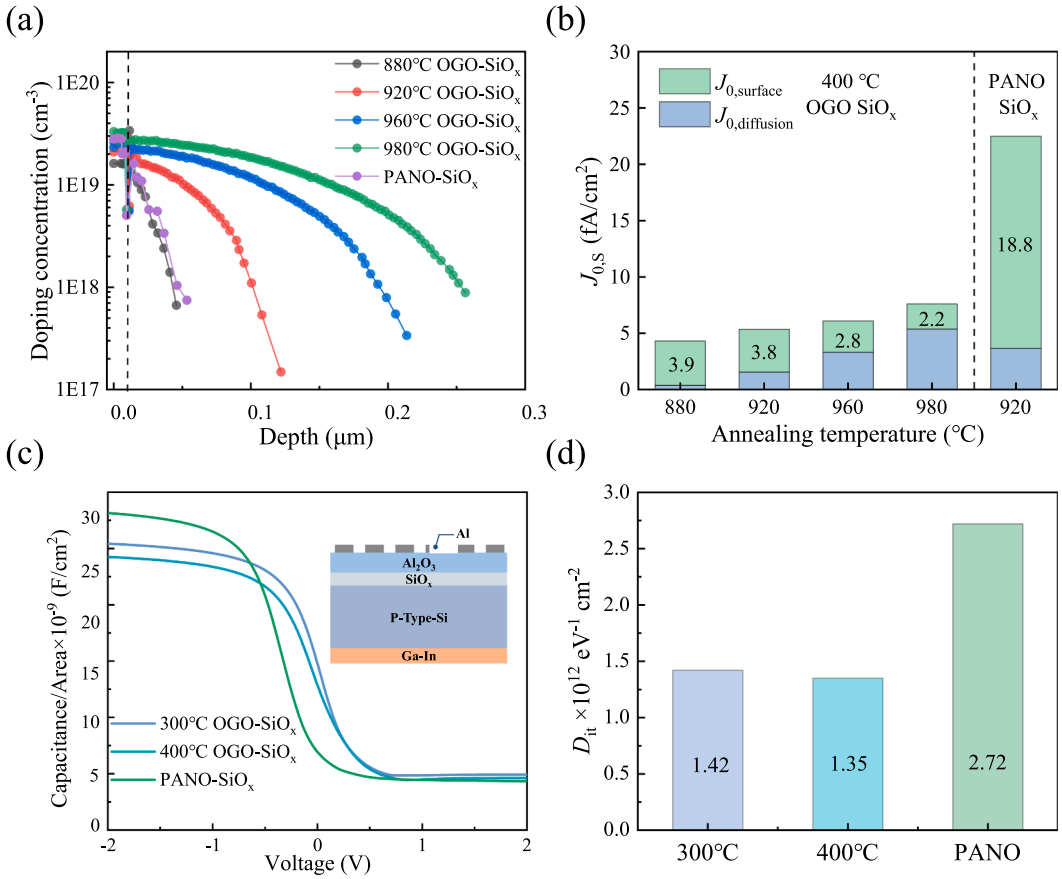

Fig. 4. (a) Active boron profiles of the PANO-SiO_x and 400 °C OGO-SiO_x samples measured by ECV under the different annealing temperature, and (b) the corresponding distribution of $J_{0,diffusion}$ and $J_{0,surface}$ calculated by EDNA2. (c) C-V curves of PANO, 300 °C and 400 °C OGO-SiO_x samples, and (d) the corresponding D_{it} values extracted from C-V curves in Fig. 4(c).

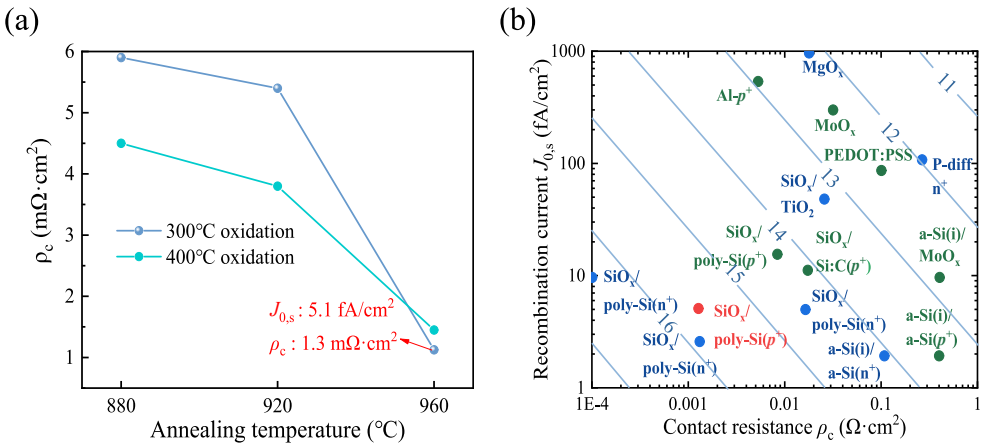

Fig. 5. (a) Contact resistivity measured by C-S method under the different annealing temperatures. (b) Selectivity factor S_{10} under the different $J_{0,s}$ and ρ_c values. Electron-selective layers are indicated by blue symbols and hole-selective layers by green symbols, while the red symbol represents the results of our study. The light blue lines represent the selectivity factor S_{10} [19]. (For interpretation of the references to colour in this figure legend, the reader is referred to the web version of this article.)

internal diffusion of B atom [9,12,15,20].

The effect of diffusion profiles of p-type TOPCon with OGO-SiO$_x$ on surface saturation current was then investigated by electrochemical capacitance–voltage (ECV) measurement combined with the numerical analyze with EDNA2 program. As shown in Fig. 4(a), the diffusion profiles of the two samples differed, with PANO-SiO$_x$ exhibiting a shallower diffusion depth than OGO-SiO$_x$. This difference may be attributed to the thicker SiO$_x$ layer in PANO-SiO$_x$, which effectively suppresses dopant diffusion. As the annealing temperature increases from 880 °C to 980 °C, the diffusion depth of OGO-SiO$_x$ to p-type TOPCon increases. A detailed numerical analysis of recombination losses was then performed by EDNA2 with the corresponding results shown in Fig. 4(b). It can be found from these result that the surface saturation current density ($J_{0,surface}$) of OGO-SiO$_x$ samples is determined to be 2.2–3.9 fA/cm^2, which is much lower than 18.8 fA/cm^2 of PANO-SiO$_x$ sample. $J_{0,surface}$ could evaluate the interface defect state, and a higher $J_{0,surface}$ means a higher SRH recombination. Therefore, the OGO-SiO$_x$ is considered to have fewer interface defects. The $J_{0,surface}$ of the OGO-SiO$_x$ sample was found to decrease as the annealing temperature increased from 880 °C to 980 °C, suggesting that higher annealing temperatures have a beneficial effect on $J_{0,surface}$. While, the higher annealing temperature would lead to deeper diffusion and more prominent SRH and Auger recombination losses, thus increase the $J_{0,diffusion}$.

We further characterized the defect states of SiO$_x$/c-Si interface using C-V measurement to extract D_{it} [16]. The test structure, based on a MOS structure, was shown in the insert of Fig. 4(c), where the sample was protected by a stable AlO$_x$ layer formed by Atomic Layer Deposition (ALD). Fig. 4(c) displays the C-V curves under the different oxidation conditions. Generally, the D_{it} can be determined by analyzing the slope of the C-V curves at a constant flat band voltage. The steeper the slope is, the higher D_{it}. In this case, it is necessary to combine the flat band voltage together with the slope to comprehensively evaluate and calculate. The calculation results show that OGO-SiO$_x$ sample has a lower D_{it} of 1.42 × 10^{12} eV^{-1}cm^{-2}, which is lower than that of PANO-SiO$_x$ with a D_{it} of 2.72 × 10^{12} eV^{-1}cm^{-2}, suggesting a lower interface defects of OGO-SiO$_x$.

In 2022, the researchers at the University of Konstanz in Germany (Konstanz) discovered that the diffusion and penetration of boron would worsen the silicon oxide, and thus lead to a marked increase in surface recombination. This phenomenon was not observed in the reference samples without boron [7]. However, we found in our previous work that the induced defects should be responsible for the poor performance of p-type TOPCon[23]. The experimental results of this study indicate that the PANO-SiO$_x$ sample displays a higher oxide integrity and shallower dopant diffusion. In that case, the PANO-SiO$_x$ should has higher passivation performance. On the contrary, the OGO-SiO$_x$ samples receive higher passivation. Therefore, even though the conclusion by Konstanz's study is reasonable, it was limited by the fact that it only investigated the effect of oxide layer integrity on passivation performance using the same technology. For silicon oxide using the different fabrication methods, controlling interfacial states is particularly important, perhaps even more important than silicon oxide integrity. Furthermore, according to our previous study, introducing carbon or nitrogen impurities when depositing poly-Si films is expected to maintain the integrity of SiO$_x$ films [14,21].

Table 3
Results are presented for selectivity $S_{10,\ e\&h,\ max}$ (top left), as well as the contact area fractions $f_{e,max}$ and $f_{h,max}$ for the electron-selective and hole-selective layers, respectively (top right and bottom left). Maximum efficiency $\eta_{e\&h,max}$ is also shown in the bottom right corner, under different conditions [19].

$S_{10,e\&h,max}$	$f_{e,max}$	Electron-selective contacts					
$f_{h,max}$	$\eta_{e\&h,max}$	OGO-SiO$_x$/ poly-Si (n^+) [15]		OGO-SiO$_x$/ poly-Si (n^+)		Th-SiO$_x$/poly-Si (n^+) [10]	
Hole-selective contacts	OGO-SiO$_x$/ poly-Si (p^+) (this work)	14.6 47.4	136.4 28.9	15.0 50.5	102.1 29.0	15.4 69.0	241.8 29.1

The contact properties of p-type TOPCon with OGO-SiO$_x$ were then checked, where two representative oxidation temperatures, i.e., 300 °C and 400 °C, were considered. As can be seen from Fig. 5(a), the contact resistivity under 880 °C annealing is below 5 mΩ·cm^2. The optimal selectivity factor of 15.6 is achieved under $J_{0,s}$ of 4.5 fA/cm^2 and ρ_c of 1.3 mΩ·cm^2 [19], which is the highest value currently reported for p-type TOPCon. Moreover, the representative TOPCon structures including p-type TOPCon and n-type TOPCon were marked in Fig. 5(b), which suggest that our p-type TOPCon shows a higher theoretical efficiency of p-type TOPCon cells. Furthermore, based on the electron selective data ($J_{0,s}$ of 0.2 fA/cm^2 and ρ_c of 2 mΩ·cm^2) in the reference [10], we predict that the limit efficiency of such a p-type TOPCon is expected to reach 29.1% as shown in Table 3.

Lastly, we fabricate the related TOPCon cells to confirm the feasibility of using p-type TOPCon to construct high-efficiency devices. The cell structure is shown in Fig. 6(a). In the process of preparing the cell, the cell before metallization was named as the precursor solar cell. Fig. 6 (b) displays the effective lifetime curves of precursor solar cell under the best oxidation and annealing temperature, where the corresponding iV_{oc}, $J_{0,s}$ and τ_{eff} values were also marked. It shows that the precursor cell achieves a high-quality passivation with an iV_{oc} of 717 mV, J_0 of 20.1 fA/cm^2, an effective lifetime of 1.8 ms and a high *iFF* of 85.2% at the injection concentration of 10^{15} cm^{-3}, and a high V_{oc} of 710 mV can be predicted. After metallization, the cell with OGO-SiO$_x$ achieves a high efficiency of 22.23% as shown in Fig. 6(c). The corresponding integrated

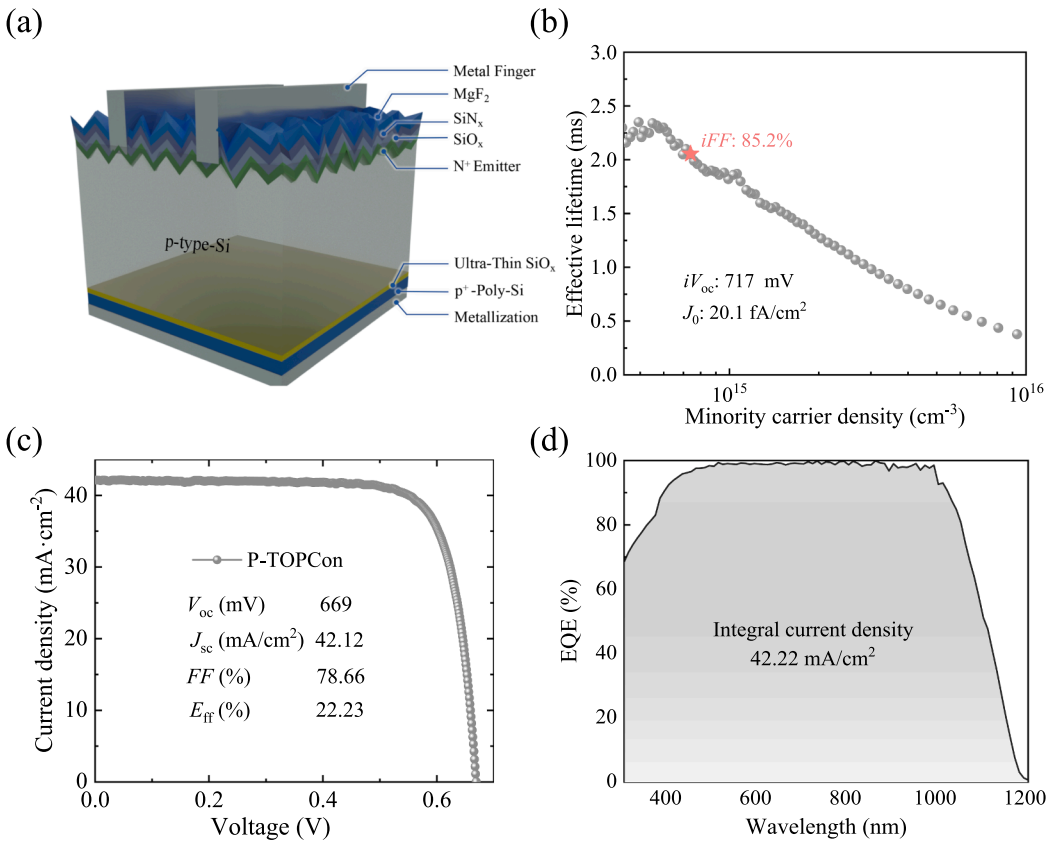

Fig. 6. Schematic structure of the p-type TOPCon SCs. (b) The effective lifetime curve of precursor SCs with the corresponding τ_{eff}, iV_{oc} and $J_{0,s}$ values were marked in this figure. (c) the current–voltage (J-V) characteristic curve, and (d) the corresponding EQE spectrum of the p-type TOPCon SCs.

current density from EQE spectrum in Fig. 6(d) was 42.22 mA/cm^2, consistent with the *J-V* curve in Fig. 6(c). The relatively low efficiency of this study can be attributed to the poor *FF* and V_{oc}, which may be caused by the metallization degeneration and metal electrode contact barriers.

4. Conclusion

In this study, we developed the p-type TOPCon constructed by OGO-SiO_x, which shows excellent passivation and contact resistivity performance. The double-sided p-type TOPCon passivated lifetime samples with p-type Si substrates achieve a highest iV_{oc} of ~ 734 mV and a lowest $J_{0,s}$ of ~ 4.5 fA/cm^2. Correspondingly, the ρ_c is below 5 mΩ·cm^2, yielding a highest S_{10} of 15.6, which is among the highest reported for p-type TOPCon SCs. The ARXPS reveals that the OGO-SiO_x thickness is 1.45 nm at 300 °C and 1.65 nm at 400 °C, revealing that the OGO-SiO_x has high oxidation ability. By combining the experiment with the numerical analysis, we can conclude that OGO-SiO_x samples show an excellent $J_{0,surface}$ of 3.9 fA/cm^2 and a lower interface defect density of 1.35×10^{12} eV^{-1}cm^{-2}, much better than that of 18.8 fA/cm^2 and 2.72×10^{12} eV^{-1}cm^{-2} of the PANO-SiO_x samples.

Finally, we fabricated the p-type Si SCs with OGO-SiO_x based p-type TOPCon passivating contact, receiving a high efficiency of 22.23%. Note that the precursor cell manifests an excellent iV_{oc} of 717 mV, indicating the potential to attain a high V_{oc} of approximately 710 mV, if the metallization process can be well-controlled. Generally, this work confirmed that OGO is a promising technology for preparing the high-quality p-type TOPCon passivating contact for industrial application.

Declaration of Competing Interest

The authors declare that they have no known competing financial interests or personal relationships that could have appeared to influence the work reported in this paper.

Acknowledgements

We would like to thank Junqian Zhizao Technology provide the free-demo ozone gas equipment. This work was supported by the Key Research and Development Program of Zhejiang Province (2021C01006), the Ningbo "Innovation 2025" Major Project (2022Z114, 2020Z098), Zhejiang Provincial Key Laboratory of Electronic Paste (2022P10009), the Science and technology projects in Liaoning Province 2021 (2021JHI/10400104), the National Nature Science Foundation of China (61974178, 61874177).

References

[1] Andreani, L.C., Bozzola, A., Kowalczewski, P., Liscidini, M., Redorici, L., 2019. Silicon solar cells: Toward the efficiency limits. Adv. Phys. 4 (1), 1548305.
[2] Chen, D., Chen, Y., Wang, Z., Gong, J., Liu, C., Zou, Y., He, Y.u., Wang, Y., Yuan, L., Lin, W., Xia, R., Yin, L.i., Zhang, X., Xu, G., Yang, Y., Shen, H., Feng, Z., Altermatt, P.P., Verlinden, P.J., 2020. 24.58% total area efficiency of screen-printed, large area industrial silicon solar cells with the tunnel oxide passivated contacts (i-TOPCon) design. Sol. Energy Mater. Sol. Cells 206, 110258.
[3] Chen, Y., Chen, D., Liu, C., Wang, Z., Zou, Y., He, Y.u., Wang, Y., Yuan, L., Gong, J., Lin, W., Zhang, X., Yang, Y., Shen, H., Feng, Z., Altermatt, P.P., Verlinden, P.J., 2019. Mass production of industrial tunnel oxide passivated contacts (i-TOPCon) silicon solar cells with average efficiency over 23% and modules over 345 W. Prog. Photovolt. 27 (10), 827–834.
[4] Cheng, H., Liu, W., Liu, Z., Yang, Z., Ma, D., Du, H., Luo, J., Xing, H., Liao, M., Zeng, Y., Yan, B., Ye, J., 2022. Emitter formation with boron diffusion from PECVD deposited boron-doped silicon oxide for high-efficiency TOPCon solar cells. Sol. Energy Mater. Sol. Cells 240, 111713.
[5] Feldmann, F., Simon, M., Bivour, M., Reichel, C., Hermle, M., Glunz, S.W., 2014. Carrier-selective contacts for Si solar cells. Appl. Phys. Lett 104 (18), 181105.
[6] Fink, C.K., Nakamura, K., Ichimura, S., Jenkins, S.J., 2009. Silicon oxidation by ozone. J. Phys. Condens. Matter 21 (18), 183001.
[7] Fırat, M., Wouters, L., Lagrain, P., Haase, F., Polzin, J.-I., Chaudhary, A., Nogay, G., Desrues, T., Krügener, J., Peibst, R., Tous, L., Sivaramakrishnan Radhakrishnan, H.,

Poortmans, J., 2022. Local Enhancement of Dopant Diffusion from Polycrystalline Silicon Passivating Contacts. ACS Appl. Mater. Inter. 14 (15), 17975–17986.
[8] Fong, K.C., Kho, T.C., Liang, W.S., Chong, T.K., Ernst, M., Walter, D., Stocks, M., Franklin, E., McIntosh, K., Blakers, A., 2018. Phosphorus diffused LPCVD polysilicon passivated contacts with in-situ low pressure oxidation. Sol. Energy Mater. Sol. Cells 186, 236–242.
[9] Gao, T., Yang, Q., Guo, X., Huang, Y., Zhang, Z., Wang, Z., Liao, M., Shou, C., Zeng, Y., Yan, B., Hou, G., Zhang, X., Zhao, Y., Ye, J., 2019. An industrially viable TOPCon structure with both ultra-thin SiO_x and n^+-poly-Si processed by PECVD for p-type c-Si solar cells. Sol. Energy Mater. Sol. Cells 200, 109926.
[10] Glunz, S.W., Steinhauser, B., Polzin, J.-I., Luderer, C., Grübel, B., Niewelt, T., Okasha, A.M.O.M., Bories, M., Nagel, H., Krieg, K., Feldmann, F., Richter, A., Bivour, M., Hermle, M., 2023. Silicon-based passivating contacts: The TOPCon route. Progr. Photovolt. 31 (4), 341–359.
[11] Guo, X., Liao, M., Rui, Z., Yang, Q., Wang, Z., Shou, C., Ding, W., Luo, X., Cao, Y., Xu, J., Fu, L., Zeng, Y., Yan, B., Ye, J., 2020. Comparison of different types of interfacial oxides on hole-selective p^+-poly-Si passivated contacts for high-efficiency c-Si solar cells. Sol. Energy Mater. Sol. Cells 210, 110487.
[12] Huang, Y., Liao, M., Wang, Z., Guo, X., Jiang, C., Yang, Q., Yuan, Z., Huang, D., Yang, J., Zhang, X., Wang, Q.i., Jin, H., Al-Jassim, M., Shou, C., Zeng, Y., Yan, B., Ye, J., 2020. Ultrathin silicon oxide prepared by in-line plasma-assisted N_2O oxidation (PANO) and the application for n-type polysilicon passivated contact. Sol. Energy Mater. Sol. Cells 208, 110389.
[13] Ingenito, A., Nogay, G., Jeangros, Q., Rucavado, E., Allebé, C., Eswara, S., Valle, N., Wirtz, T., Horzel, J., Koida, T., Morales-Masis, M., Despeisse, M., Haug, F.J., Löper, P., Ballif, C., 2018. A passivating contact for silicon solar cells formed during a single firing thermal annealing. Nat. Energy 3, 800–808.
[14] Lin, Y., Yang, Z., Liu, Z., Zheng, J., Feng, M., Zhi, Y., Lu, L., Liao, M., Liu, W., Ma, D., Han, Q., Cheng, H., Zeng, Q., Yuan, Z., Yan, B., Zeng, Y., Ye, J., 2021. Dual-functional carbon-doped polysilicon films for passivating contact solar cells: Regulating physical contacts while promoting photoelectrical properties. Energy Environ. Sci 14 (12), 6406–6418.
[15] Liu, Z., Lin, N.a., Zhang, Q., Yang, B., Xie, L., Chen, Y., Li, W., Liao, M., Chen, H., Liu, W., Wang, Y., Huang, S., Yan, B., Zeng, Y., Wan, Y., Ye, J., 2022. 24.4% industrial tunnel oxide passivated contact solar cells with ozone-gas oxidation Nano SiOx and tube PECVD prepared in-situ doped polysilicon. Sol. Energy Mater. Sol. Cells 243, 111803.
[16] Ma, D., Liu, W., Xiao, M., Yang, Z., Liu, Z., Liao, M., Han, Q., Cheng, H., Xing, H., Ding, Z., Yan, B., Wang, Y., Zeng, Y., Ye, J., 2022. Highly improved passivation of PECVD p-type TOPCon by suppressing plasma-oxidation ion-bombardment-induced damages. Sol. Energy 242, 1–9.
[17] Polzin, J.-I., Lange, S., Richter, S., Moldovan, A., Bivour, M., Hagendorf, C., Hermle, M., Glunz, S.W., Feldmann, F., 2020. Temperature-induced stoichiometric changes in thermally grown interfacial oxide in tunnel-oxide passivating contacts. Sol. Energy Mater. Sol. Cells 218, 110713.
[18] Richter, A., Benick, J., Feldmann, F., Fell, A., Hermle, M., Glunz, S.W., 2017. n-Type Si solar cells with passivating electron contact: Identifying sources for efficiency limitations by wafer thickness and resistivity variation. Sol. Energy Mater. Sol. Cells 173, 96–105.
[19] Schmidt, J., Peibst, R., Brendel, R., 2018. Surface passivation of crystalline silicon solar cells: Present and future. Sol. Energy Mater. Sol. Cells 187, 39–54.
[20] Tong, H., Liao, M., Zhang, Z., Wan, Y., Wang, D., Quan, C., Cai, L., Gao, P., Guo, W., Lin, H., Shou, C., Zeng, Y., Yan, B., Ye, J., 2018. A strong-oxidizing mixed acid derived high-quality silicon oxide tunneling layer for polysilicon passivated contact silicon solar cell. Sol. Energy Mater. Sol. Cells 188, 149–155.
[21] Yang, Q., Liu, Z., Lin, Y., Liu, W., Liao, M., Feng, M., Zhi, Y., Zheng, J., Lu, L., Ma, D., Han, Q., Cheng, H., Yang, Z., Ding, K., Duan, W., Chen, H., Wang, Y., Zeng, Y., Yan, B., Ye, J., 2021. Passivating Contact with Phosphorus-Doped Polycrystalline Silicon-Nitride with an Excellent Implied Open-Circuit Voltage of 745 mV and Its Application in 23.88% Efficiency TOPCon Solar Cells. Sol. RRL 5, 202100644.
[22] Young, D.L., Lee, B.G., Fogel, D., Nemeth, W., LaSalvia, V., Theingi, S., Page, M., Young, M., Perkins, C., Stradins, P., 2017. Gallium-Doped Poly-Si:Ga/SiO_2 Passivated Emitters to n-Cz Wafers with IV_{oc} >730 mV. IEEE J Photovolt. 7, 1640–1645.
[23] Zeng, Y., Ma, D., Liu, Z., Liao, M., Xiao, M., Xing, H., Lin, N.a., Ding, Z., Cheng, H., Wang, Y., Liu, W., Yan, B., Ye, J., 2022. Effects of PECVD preparation conditions and microstructures of boron-doped polysilicon films on surface passivation of p-type tunnel oxide passivated contacts. Mat. Sci. Semicon. Proc. 150, 106966.
[24] Zhang, Z., Liao, M., Huang, Y., Guo, X., Yang, Q., Wang, Z., Gao, T., Shou, C., Zeng, Y., Yan, B., Ye, J., 2019. Improvement of Surface Passivation of Tunnel Oxide Passivated Contact Structure by Thermal Annealing in Mixture of Water Vapor and Nitrogen Environment. Sol. RRL 3 (10), 1900105.
[25] Zhi, Y., Zheng, J., Liao, M., Wang, W., Liu, Z., Ma, D., Feng, M., Lu, L., Yuan, S., Wan, Y., Yan, B., Wang, Y., Chen, H., Yao, M., Zeng, Y., Ye, J., 2021. Ga-doped Czochralski silicon with rear p-type polysilicon passivating contact for high-efficiency p-type solar cells. Sol. Energy Mater. Sol. Cells 230, 111229.